Available online at www.sciencedirect.com
SCIENCE DIRECT
Polymer 46 (2005) 9329–9341
polymer
www.elsevier.com/locate/polymer

Rapid formation of soft hydrophilic silicone elastomer surfaces

Kirill Efimenko[a], Julie A. Crowe[a], Evangelos Manias[b], Dwight W. Schwark[c], Daniel A. Fischer[d], Jan Genzer[a,*]

[a]*Department of Chemical and Biomolecular Engineering, North Carolina State University, Raleigh, NC 27695-7905, USA*
[b]*Department of Materials Science and Engineering, Pennsylvania State University, University Park, PA 16802, USA*
[c]*Sealed Air, Cryovac Food Packaging Division, Duncan, SC 29334, USA*
[d]*Materials Science and Engineering Laboratory, National Institute of Standards and Technology, Gaithersburg, MD 20899, USA*

Received 30 April 2005; received in revised form 9 July 2005; accepted 14 July 2005
Available online 10 August 2005

Abstract

We report on the rapid formation of hydrophilic silicone elastomer surfaces by ultraviolet/ozone (UVO) irradiation of poly(vinylmethyl siloxane) (PVMS) network films. Our results reveal that the PVMS network surfaces render hydrophilic upon only a short UVO exposure time (seconds to a few minutes). We also provide evidence that the brief UVO irradiation treatment does not cause dramatic changes in the surface modulus of the PVMS network. We compare the rate of formation of hydrophilic silicone elastomer surfaces made of PVMS to those of model poly(dimethyl siloxane) (PDMS) and commercial-grade PDMS (Sylgard-184). We find that relative to PVMS, 20 times longer UVO treatment times are needed to oxidize the PDMS network surfaces in order to achieve a comparable density of surface-bound hydrophilic moieties. The longer UVO treatment times for PDMS are in turn responsible for the dramatic increase in surface modulus of UVO treated PDMS, relative to PVMS. We also study the formation of self-assembled monolayers (SAMs) made of semifluorinated organosilane precursors on the PVMS-UVO and PDMS-UVO network surfaces. By tuning the UVO treatment times and by utilizing mono- and tri-functional organosilanes we find that while mono-functionalized organosilanes attach directly to the substrate, SAMs of tri-functionalized organosilanes form in-plane networks on the underlying UVO-modified silicone elastomer surface, even with only short UVO exposure times.

Keywords: Functionalized silicone rubber; Surface modification; Self-assembly

1. Introduction

The production of surfaces with tailored physico-chemical characteristics is the goal of many research investigations for technological applications including lubricated bearing surfaces, antifouling coatings, non-staining textiles, adhesives, or paints. When designing and fabricating surfaces with specific characteristics, one has to always consider that surface functional groups are subject to the dynamic properties of the material. While multiple chemical routes exist that lead to reproducible control of surface functional groups, which impact the wettability and mechanical properties of materials, our ability to tailor the surface dynamics is still rather limited.

It has been recognized that polymeric surfaces are good candidates for controlling the mobility of the surface functional groups. Over the past several years, great advances have been made in designing 'smart'/responsive polymer surfaces [1,2]. Koberstein and coworkers have designed a series of smart polymeric surfaces based on synthetic polymers tailored with various end-groups that have a broad range of lyophobicity ranging from carboxylic acid to fluorine-containing moieties [3,4]. Similar strategies have been adopted by Anastasiadis and coworkers who studied surface reorganization in polystyrene/polyisoprene copolymers modified with either dimethylamine or sulfo-betaine end-groups [5]. The researchers demonstrated that the polymer's terminal functional groups respond to outside environmental changes where its favored state is either at the surface due to attractive forces or 'hiding' just beneath it due to repulsive forces. From a practical point of view, the rather high glass transition temperature (T_g) of the polymers employed prolonged the system's response time to the outside environment from hours to days.

* Corresponding author. Tel.: +1 919 515 2069.
E-mail address: jan_genzer@ncsu.edu (J. Genzer).

0032-3861/$ - see front matter © 2005 Elsevier Ltd. All rights reserved.
doi:10.1016/j.polymer.2005.07.046

An alternative strategy in designing responsive surfaces has been adopted by Ferguson and coworkers. They have utilized simple chemical oxidation routes on cross-linked commercially available polybutadienes (PBD) in order to generate hydrophilic functional groups within the PBD network [6]. These oxidized polybutadiene (PBD-ox) surfaces rearranged within several minutes when exposed to polar media, such as water. This quick response was attributed to PBD's low T_g, which allows for the chains' configurational flexibility in reconstruction. Ferguson and coworkers also showed that temperature had a pronounced effect on the conformation of PBD-ox [7–10]. Specifically, at low temperatures the chain conformation was controlled by the system enthalpy, as the number of the hydrophilic moieties present at the polymer/water interface was maximized. Conversely, at high temperatures entropic restoring forces prevailed as the chains in the cross-linked network adopted a coil-like conformation thus reducing surface hydrophilicity. The responsive behavior was reversible over many temperature cycles.

This brief overview leads to evaluating two primary parameters that can influence surface reconstruction: (i) The nature of the functional groups present at the polymer and (ii) the polymer flexibility. Ideally, the latter can be accomplished by using networks of polymeric liquids with a low T_g. In such a situation, the segments of the chains are locally very mobile but because they are a part of a network, the chains' translational mobility is limited and the system maintains a solid shape.

Silicone elastomers (SEs) represent a unique class of materials. When chemically cross-linked, SEs form flexible networks with an elastic modulus of $\approx$1 MPa [11]. Most SEs possess a low T_g; for example the glass transition of the common poly(dimethyl siloxane) (PDMS) elastomer is $\approx$150 K [12]. The high flexibility of the Si–O backbone assures that SEs can readily adopt the lowest surface energy conformations while responding to changes of environment. For example, when in contact with air, the pendant methyl groups in PDMS are closely packed at the air interface resulting in a hydrophobic surface. When in contact with water, however, the dipole of the siloxane backbone is the dominant interaction between the two media and its surface becomes more hydrophilic [13].

Over the past several years, a variety of bulk [14] and surface [15,16] modifications of PDMS have been explored using various techniques that involved either physical [17–19] or chemical treatment, [20] or the combination of both [16,21]. In particular, oxygen plasma treatment of PDMS has been widely used to generate a hydrophilic surface as confirmed by X-ray photoelectron spectroscopy [22]. Studies utilizing this method reported irreversible chemical changes in the near-surface region of PDMS propagating several hundred nanometers deep into the sample [17,23,24]. This treatment converted the PDMS surface 'skin' into a thin and brittle silica-like layer affecting the elastomer's mechanical properties. Owen and Smith reported on the formation of cracks in the silica-like layer and argued that the cracks allowed for the migration of low molecular weight uncross-linked PDMS fragments to the surface, a phenomenon termed 'hydrophobic recovery' [23]. Another class of techniques used extensively to modify PDMS surfaces involves ultraviolet (UV) [25–27] and UV/ozone irradiation (UVO) [28,29]. Although the processing time is an order of magnitude slower, silicone rubbers still undergo dramatic surface chemical changes similar to those induced by the oxygen plasma when exposed to UV light or the combination of UV light and ozone. Numerous research groups have used contact angle techniques to confirm that the UVO-modified PDMS surfaces were polar; being comprised primarily of surface bound –OH groups, although non-negligible traces of carbon containing species were also detected with X-ray photoelectron spectrometry even after very long treatment times [29]. The same researchers also reported on ellipsometric measurements on UVO-modified PDMS and argued that a uniform silica-like layer was created on the irradiated surface with a thickness around 10–30 nm.

To date, Efimenko and co-workers have performed the most comprehensive study of the UVO-modification of PDMS [30]. The effects of the UV light wavelength and ambient conditions on the surface properties of industrial grade PDMS composite (Sylgard-184, Dow Corning) were probed using a battery of experimental probes, including static contact angle measurements, Fourier transform infrared spectroscopy, near-edge X-ray absorption fine structure spectrometry, and X-ray reflectivity. The results revealed that when exposed to UV, the PDMS macromolecules in the surface region of Sylgard-184 underwent chain scission of both the main chain backbone and the side-groups in the network. The radicals formed during this process recombined and formed a network whose wetting properties were similar to those of a UV-modified model PDMS. In contrast to UV radiation, UVO treatment causes very significant changes in the surface and near-surface structure of Sylgard-184. Specifically, the molecular oxygen and ozone created during the UVO process interacted with the UV-modified specimen. As a result of these interactions, the surface of the sample contained a large number of hydrophilic (mainly –OH) groups. In addition, the material density within the first $\approx$5 nm reached about 50% of that of pure silica. While more controlled than the plasma treatment, the UVO modification of PDMS may still cause uncontrollable changes to the surfaces of SEs. In particular, long time exposure of PDMS to UVO creates almost a rigid silica-like layer on the surface of the PDMS [30]. While in some cases this is beneficial, such as in the formation of a topographically resolved surface, [31], it is averse to creating a soft hydrophilic surface layer.

In order to overcome this obstacle, one would need to alter the chemical structure of the SEs and/or decrease the UVO treatment time. The aim of this work is to show that

this task can be accomplished by replacing PDMS networks with poly(vinyl methyl siloxane) (PVMS) networks. We provide experimental evidence, in contrast to the UVO modification of PDMS, which render hydrophilic only after prolonged UVO modification, that only brief UVO treatment times (seconds to a few minutes) are sufficient to form highly hydrophilic SE surfaces. Experiments aimed at probing the mechanical properties of the PVMS-UVO surfaces reveal that UVO-treatment times of seconds to minutes does not dramatically alter the surface modulus of PVMS. The PVMS-UVO surfaces retain their soft, elastic nature. The ability to fine-tune the concentration of the hydrophilic moieties on the UVO-treated SE surfaces is utilized in studying the structure of self-assembled monolayers (SAMs) made of semifluorinated organosilane precursors. Specifically, we will demonstrate that while mono-functionalized organosilanes attach directly to the UVO-activated SE substrate, SAMs of tri-functionalized organosilanes form in-plane networks on the underlying UVO-modified SE.

2. Materials and methods

2.1. Synthesis of poly(vinyl methyl siloxane) and network formation

PVMS was synthesized in house using either equilibrium-controlled or kinetically-controlled ring opening polymerization (ROP) and step-growth polymerization methods. In the first step, vinyl methyl dichlorosilane was dissolved in a dilute aqueous solution of HCl to form a mixture of short oligomeric vinyl methyl siloxane chains and cyclic structures comprising $[Si(CH{=}CH_2)CH_3{-}O]_n$, where n ranged from 3 to about 6 [32,33]. In the second step, the cyclic structures were separated by vacuum distillation with an optimal yield up to 60–70%. In step-growth polymerization (method A), short-chain silanols were condensed until the desired polymer chain was reached. The reaction proceeds under mild basic conditions and the condensing water must be removed for increases in molecular weight. The reaction was monitored for viscosity changes and can be stopped by neutralization of the catalyst. The advantages of this route include an available source of the short-chain silanols, very high yield of the polymer (almost 98%), and the flexibility to obtain PVMS with a large range of molecular weight (by varying the reaction times). In kinetically controlled ROP (method B), the controlled growth of the propagating chain results in a very narrow polydispersity over a wide range of molecular weights. In this case, we synthesize the starting monomer—trivinylmethyl cyclosiloxane—as it is not widely available and the larger ring (tetra- or penta-) analogs do not have the necessary ring-strain for efficient polymerization. The reaction was initiated with either a hard mono-functional cation, such as n-butyl lithium, or a bifunctional initiator like lithium dimethylsiloxanolate $(LiOSiMe_2)O$ in the presence of an aprotic solvent (THF, DMSO, etc.) in order to loosen the ion–ion pair interactions for efficient polymerization [34,35]. To terminate the reaction, the active propagating center was end-capped with the addition of acetic acid to form the lithium acetate salt and the –OH terminus (Scheme 1) [34,36–40].

PVMS fluids with several molecular weights were synthesized and characterized by IR spectroscopy and size exclusion chromatography (SEC). The IR spectroscopy, performed in the transmission mode, confirmed the presence of the vinyl functionalities. The molecular weight of PVMS synthesized from 3-member cyclic VMS was measured by SEC equipped with several detectors: Refractive index (RI), UV, light scattering, and viscosity. The viscosity data were used to evaluate the molecular weight of the polymer. In a separate set of experiments, we have measured the viscosity of PVMS as a function of the shear rate. For each molecular weight, the viscosity remained constant over a range of shear rates (which varied over more than two orders of magnitude in s^{-1} for each molecular weight). The viscosity data were then used to generate a calibration curve for the molecular weight of PVMS versus polymerization time for both types of polymerizations.

The key to our high-density surface modification of the substrate is to cross-link PVMS chains only at reactive terminal ends. This preserves the active vinyl group on the silicon for post-modification. We have utilized the standard alkoxy condensation routes for network formation by reacting the silanol-terminated PVMS with tetraethoxysilane (TEOS), as the cross-linker. Typically, the mixture of PVMS, TEOS and the tin-based catalyst was poured into a plastic Petri dish and post-cured under vacuum at 50 °C for 48 h to ensure complete cross-linking. Rheological experiments revealed that the optimum stoichiometric TEOS: PVMS ratio leading to films with the highest elasticity was about 1.7:1. The finding that an excess of cross-linker is necessary to yield highest elasticity is in accord with previous work of Cohen and coworkers carried out with PDMS [41]. Before use, the PVMS networks were Soxhlet extracted in toluene for 48 h, blow dried with nitrogen and vacuum dried at 70 °C for additional 48 h.

We also prepared a set of PDMS networks based on commercial grade Sylgard-184. The methodology was the same as that described in our previous publication [30]. As Sylgard-184 is formulated with silica and other reinforcing fillers, we also prepared model PDMS networks containing no fillers for direct comparison to our PVMS networks. The model PDMS networks were formed by cross-linking vinyl-terminated PDMS ($M_n \approx 49.5$ kDa) with tetrakis (dimethylsiloxy) silane using standard hydrosilation in the presence of Pt catalyst. Both PDMS networks were Soxhlet extracted in toluene for 48 h, blow dried with nitrogen and vacuum dried at 70 °C for additional 48 h.

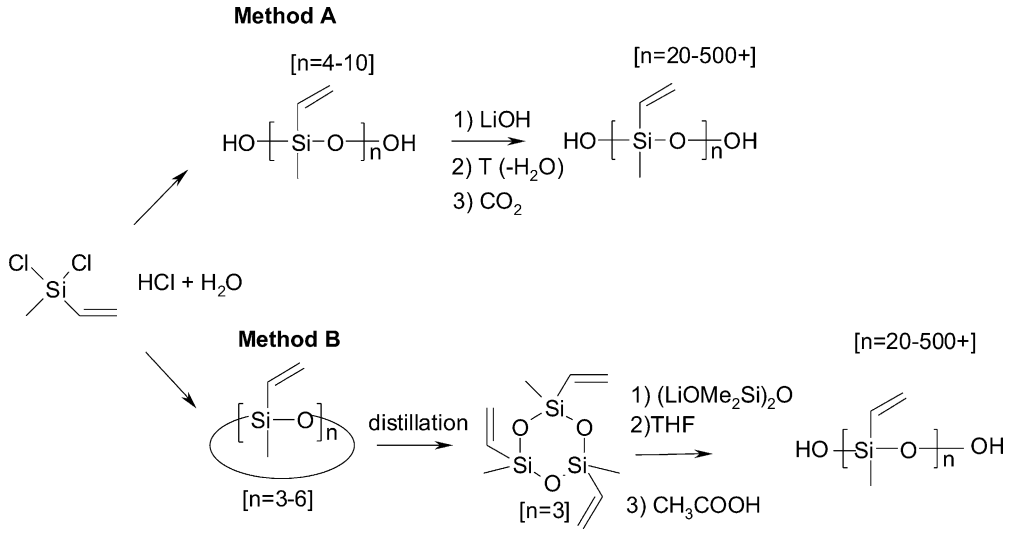

Scheme 1. Chemical routes leading towards the synthesis of PVMS.

2.2. Ultraviolet/ozone (UVO) treatment

The ultraviolet/ozone (UVO) treatment of the PVMS surface was carried out in a commercial UVO chamber (Jelight Company, Inc., model 42) [42]. The UVO treatment is a photosensitized oxidation process in which the molecules of the treated material are excited and/or dissociated by the absorption of short-wavelength UV radiation. Atomic oxygen is simultaneously generated when molecular oxygen is dissociated by $\lambda_1 = 184.9$ nm and ozone by $\lambda_2 = 253.7$ nm. The 253.7 nm radiation is absorbed by most hydrocarbons and also by ozone. The organic products of this excitation react with atomic oxygen to form simpler, volatile molecules, which desorb from the surface. Therefore, when both wavelengths are present, atomic oxygen is continuously generated, and ozone is continually formed and destroyed. We used the standard Fused Quartz lamp that transmits about 65% of radiation at 184.9 nm and has an output of 28 mW/cm^2 at the distance 6 mm, as reported by the manufacturer. The PVMS specimens were placed onto glass slides and put into the UVO-cleaner tray at the distance of about 5 mm from the UV-source and exposed to the radiation from one side only for controlled periods of time. The pressure, temperature, and relative humidity in the chamber were maintained at 1 atm, 20 °C, and 50–60%, respectively.

2.3. Formation of semifluorinated self-assembled monolayers

1H,1H,2H,2H-Perfluorodecyl dimethylchlorosilane (*m*-F8H2) and 1H,1H,2H,2H-perfluorodecyl trichlorosilane (*t*-F8H2), both supplied by Lancaster and used as received, were used to form semifluorinated (SF) self-assembled monolayers (SAMs) on top of the UVO-treated PVMS films. A small amount of a given SF chlorosilane was placed on the bottom of a petri dish, a silicon wafer covered with UVO-treated and cross-linked PVMS was positioned above the SF chlorosilane source (distance ≈ 1 cm), the whole system was closed and kept at ambient conditions. After 15 min the substrate was taken out of the container, washed thoroughly with ethanol to remove any physisorbed SF chlorosilane molecules and completely dried with nitrogen.

2.4. Contact angle measurements using the sessile drop technique

The contact angle experiments were performed with deionized (DI) water ($R > 15$ MΩ cm) using a Ramé-Hart contact angle goniometer (model 100-00) equipped with a CCD camera, and analyzed with the Ramé-Hart Imaging 2001 software [42]. The contact angles were read as a function of time after depositing 8 μL of the probe liquid on the substrate. Each data point reported in the paper represents an average over three to five measurements on different areas of the same sample and has an error less than $\pm 1.5°$.

2.5. Fourier transform infrared spectroscopy in the attenuated total reflection mode

Fourier transform infrared spectroscopy in the attenuated total reflection mode (FTIR-ATR) was used for characterizing chemical changes that took place on the surface of the polymer. The spectra were recorded on Digilab UMA-500 spectrometer equipped with liquid nitrogen cooled MCT detector and the mirror speed was set at 0.3 cm/s [42]. For each sample, 2048 scans were collected using Ge-crystal detector with a resolution of 4 cm^{-1} under constant nitrogen flux to eliminate the effect of water vapor on the collected data. The data were analyzed using BioRad-IR software [42].

2.6. Near-edge X-ray absorption fine structure

We used near-edge absorption fine structure (NEXAFS) spectroscopy to examine the surface chemistry of the PVMS-UVO samples. We also utilized NEXAFS spectroscopy to detect the presence of semifluorinated SAMs deposited on top of the PVMS-UVO specimens. The NEXAFS experiments were carried out at the NIST/Dow Soft X-ray materials characterization facility of the national synchrotron light source (NSLS) at Brookhaven National Laboratory [43,44]. NEXAFS involves the resonant soft X-ray excitation of a K or L shell electron to an unoccupied low-lying antibonding molecular orbital of σ symmetry, σ*, or π symmetry, π* [45]. The initial state K shell excitation gives NEXAFS its element specificity, while the final-state unoccupied molecular orbitals provide NEXAFS with its bonding or chemical selectivity. A measurement of the partial electron yield (PEY) intensity of NEXAFS spectral features thus allows for the identification of chemical bonds and determination of their relative population densities on the surface of the sample (≈2 nm probing depth). All spectra were collected at $\theta = 50°$, where θ is the angle between the sample normal and the polarization vector of the X-ray beam [46,47].

2.7. Surface modulus measurement

The elastic modulus of bare PVMS and PVMS-UVO was measured by indentation experiments using atomic force microscopy (AFM, Digital Instruments Nanoscope III) operated at a force-distance mode [48] and utilizing only the first 5 nm of compression, isolating the modified-surface modulus [49,50] (the top 10–30 nm of the irradiated surface are distinct in nature from underlying elastomeric material). Both loading and unloading curves were collected and analyzed [51], yielding the same values for the compressive surface modulus. The moduli reported herein were derived from the unloading curves and for the first 5 nm of compression, measured in at least five different spots on each sample. To obtain accurate relative moduli, all measurements were performed with the same cantilever and tip, and neat (=untreated) PVMS elastomer was used as a reference. Subsequent calibration of the cantilever's normal spring constant also provided absolute values for moduli [48]. Both a sharp Si_3N_4 AFM tip as well as a tungsten sphere (diameter ≈10 μm) attached on the tip of same cantilever, were employed in these tests, giving the same results for the elastic modulus values reported herein.

3. Results and discussion

We first examined the surfaces of bare PVMS network films by depositing a droplet of water (≈8 μL) and monitoring the time dependence of the contact angle. In Fig. 1 we plot the dependence of deionized (DI) water contact angle (CA) on time (t) for model PDMS networks (solid squares), Sylgard-184 networks (open squares), and bare PVMS networks (solid circles).

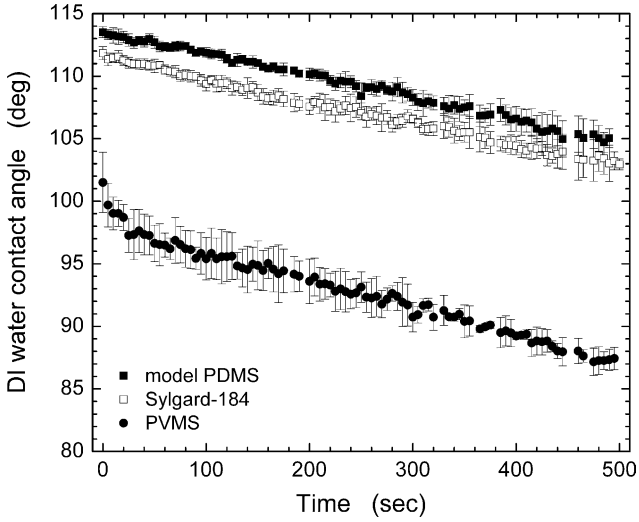

Fig. 1. Time dependence of water contact angle measured on model PDMS networks (solid squares), Sylgard-184 networks (open squares), and bare PVMS networks (solid circles). The error bars represent an average over three measurements performed on three different areas of the same sample.

The data shown represent an average over three measurements performed on three different areas of the same specimen. In all three cases, there is a decrease in the contact angle with increasing time. Recent reports utilizing dynamic contact angle reveal that the surface wettability stays constant [52]. In our sample, we noticed that the volume drop size was changing throughout the experiment. Detailed analysis of the data revealed that while the drop diameter remained essentially unchanged, there was a steady decrease in the height of the drop. We thus attribute this behavior to the evaporation of water from the probing droplet. One can get initial insight into the response of the surface to the presence of water by monitoring the time dependence of the dCA/dt slope (cf. Fig. 2). The results presented in Figs. 1 and 2 reveal that the PDMS surfaces are relatively hydrophobic throughout the entire measurement. There is a small difference between the degree of hydrophobicity between the two PDMS samples. We speculate that the slightly increased hydrophilicity of Sylgard-184 relative to the model PDMS network is associated with the presence of the fillers and resins contained in the commercial grade SE. The behavior of PVMS is different from that of PDMS. Specifically, the contact angle is initially lower than that of PDMS. Considering that relative to the methyl group, the vinyl functionality has a higher surface energy than the methyl functionality, this result indicated that the surface of PVMS comprises a mixture of both groups. When placed in contact with DI water, the contact angle changes initially rapidly from higher to lower values and then saturates at times longer than about 30 s. This behavior indicates that as soon

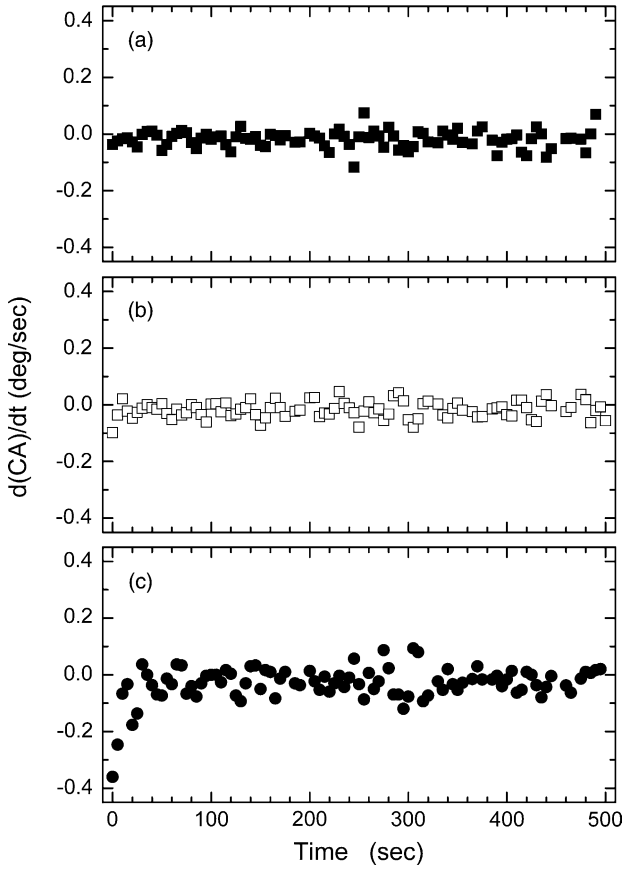

Fig. 2. Change of the contact angle with increasing time for model PDMS networks (solid squares), Sylgard-184 networks (open squares), and bare PVMS networks (solid circles).

as water comes into contact with the PVMS surface, the system minimized its free energy by increasing the number of higher surface energy vinyl groups at the PVMS/water interface.

The rapid decrease in the contact angle, associated with the aforementioned rearrangements of the functionalities on the PVMS surface, is a consequence of the high flexibility of the Si–O bond. It is worth comparing the current results to those reported in the literature. For example, Koberstein and coworkers reported rates of surface rearrangement to vary from hours to days, depending on the system under investigation [1,3,4]. Anastasiadis et al. observed response times on the order of hours [5]. Ferguson and coworkers detected surface rearrangement rates on the order of minutes on oxidized polybutadienes [6–10]. To the best of our knowledge, the rate at which the PVMS network surface reorients represents the fastest surface response observed in any polymer-based material.

One of the goals of this work is to develop a robust and efficient way of generating hydrophilic silicone elastomers by activating the vinyl functionality in PVMS. One can generate hydrophilic functionalities, such as alcohols and carboxylic acids, by oxidation using, for example, permanganate, as reported by Ferguson [6–10]. Alternatively, specific functionalities can be reacted with the vinyl bond using the thiol-ene addition reaction, a mechanism successfully employed for modification of vinylmethyl-*co*-dimethylsiloxanes fluids [53–56]. To obtain amphiphilic block siloxane copolymers, Chojnowski et al. transformed $>90\%$ of the pendant vinyl groups with the free radical addition of mercaptoacetic acid. Initiated via thermal or photochemical means, it has been demonstrated that the reaction follows the anti-Markovnikov rule resulting in the β-adduct copolymers [54,55]. The thiol-ene addition reaction has also been exploited by Ferguson's work with 1,2 PBD surfaces [6]. Surface treatment experiments with both the chemical oxidation and thiol-ene addition methodologies on our PVMS networks are underway and will be reported separately. In this work, we generate the hydrophilic functionalities by utilizing the UVO treatment.

The UVO-modified PVMS samples (PVMS-UVO) were obtained using the UVO treatment procedure outlined in the methods section. The variation in the surface chemistry was monitored using FTIR-ATR measurements. In the main part

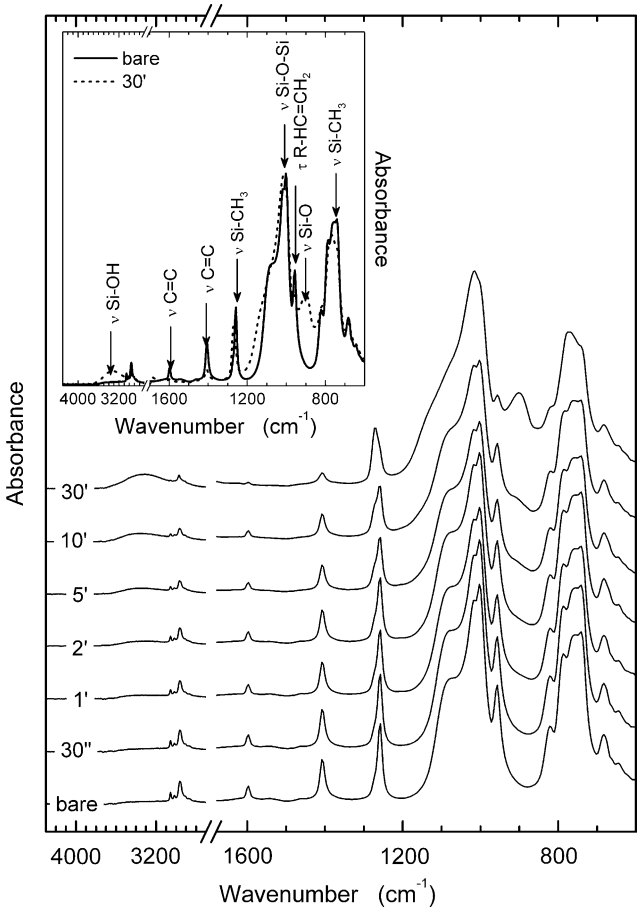

Fig. 3. FTIR-ATR spectra from extracted PVMS samples treated with UVO for various times ranging from 0 to 30 min. The arrows in the figure mark the positions of some characteristic IR bands (see text for details). The spectra have been shifted vertically for clarity. The inset shows the FTIR-ATR spectra from bare PVMS (solid line) and the PVMS-UVO treated for 30 min (dashed line).

of Fig. 3 we plot a sequence of IR spectra for PVMS-UVO samples treated for various UVO times. PVMS exhibits a series of characteristic IR bands (Table 1) [57]. Among the most intense are those associated with $-CH_3$ rocking and ≡Si–C≡ stretching (≈785–815 cm^{-1}), asymmetric Si–O–Si stretches (≈1055–1090 cm^{-1}), symmetric $-CH_3$ deformations (≈1245–1270 cm^{-1}), and asymmetric $-CH_3$ stretches (≈2950–2970 cm^{-1}). In addition, a number of peaks indicate the presence of the vinyl functionality, such as C=C twist/$=CH_2$ wagging (≈960 cm^{-1}), $=CH_2$ scissors (≈1407 cm^{-1}), C=C stretch (≈1587 cm^{-1}), and C=C wagging (≈1900 cm^{-1}).

The UVO-treated PVMS contains additional peaks, such as ≡Si–OH stretching (≈875–920 cm^{-1}) and asymmetric Si–OH stretches (≈3050–3700 cm^{-1}). In the inset to Fig. 3, we plot the IR spectra of bare PVMS (solid line) and the PVMS-UVO treated for 30 min (dashed line). By inspecting the IR spectra in Fig. 3 several conclusions can be made about the UVO modification of PVMS. With increasing UVO treatment time, there is a decrease in the bands whose intensity is characteristic of the vinyl functionality; this is accompanied with an increase in the Si–OH signal. There does not seem to be a decrease of the Si–O–Si, which would be a signature of chain scission occurring during the UVO treatment. Thus the short UVO treatment leads to oxidative conversion of vinyl functionalities on PVMS into more hydrophilic species, such as hydroxyls.

It is worth noting that this behavior is different from that we reported previously on UVO treatment of PDMS [30]. Specifically, we observed that substantial chain scission occurred during the UVO treatment of commercial silicone elastomer Sylgard-184. We also observed that in Sylgard-184, chain scission was accompanied with the creation of short hydrocarbon linkages in the UVO-modified Sylgard-184 samples [58]. Presumably, relative to the Si–O–Si linkage, the $-CH{=}CH_2$ bond has a higher susceptibility to the UVO treatment [29].

Because of the rather poor surface sensitivity relative to other techniques, FTIR-ATR cannot be used to monitor the depth distribution of the functional groups in the sample.

Table 1
Assignment of IR spectra of PVMS shown in Fig. 3.

IR region (cm^{-1})	Description
785–815	$-CH_3$ rocking and ≡Si–C≡ stretching in ≡Si–CH_3
825–865	≡Si–O stretch in ≡Si–OH
875–920	≡Si–O stretch in ≡Si–OH
960	C=C twist/$=CH_2$ wagging
1055–1090	Asymmetric ≡Si–O–Si≡ stretch
1245–1270	Symmetric $-CH_3$ deformation in ≡Si–CH_3
1407	$=CH_2$ scissors
1587	C=C stretch
1900	C=C wagging
2950–2970	Asymmetric $-CH_3$ stretch in ≡Si–CH_3
3050–3700	–OH stretching in ≡Si–OH, possibly also in ≡C–OH (3610–3640 cm^{-1})

Hence, in order to confirm that the changes detected with FTIR-ATR reported above indeed occurred primarily on the surface of the PVMS network, we performed NEXAFS spectroscopy experiments and detected the partial electron yield, which comprises Auger electron signal that originates from the first ≈10 nm thick sub-surface region in the sample. In Fig. 4 we present the partial energy yield (PEY) NEXAFS spectra at the carbon K-edge collected from for PVMS samples with $M_n = 34$ kDa (a) and $M_n = 49$ kDa (b) treated for various UVO times ranging from 0 to 30 min. All spectra contain strong peaks around 287 and 290 eV, which are characteristic signatures of $1s \rightarrow \sigma^*$ transitions of the C–H and C–C bonds, respectively. In addition, the spectra from the bare PVMS samples contain a peak at ≈283 eV, which represent the $1s \rightarrow \pi^*$ transition in the C=C bond characteristic of the vinyl functionality in PVMS. By increasing UVO treatment time, we observe a decrease in the intensity of the $1s \rightarrow \pi^*$ transition indicating the disappearance of the surface-vinyl functionality. Simultaneously, there is an intensity increase of the second harmonic oxygen signal (≈260–285 eV). This indicates that the UVO-treated surfaces contain a large number of oxygen-bearing species. Based on the FTIR-IR spectra, we attribute this to the increased presence of hydroxyl groups at the sample's surface.

From the data in Fig. 4, the amount of the 'oxygen-containing' species increases with increasing UVO-treatment time. This is indicated by the strong increase in the second harmonic oxygen signal. Interestingly, the amount of these functionalities seems to depend on the molecular weight of PVMS, or alternatively on the cross-link density of the network. Our results reveal that the concentration of the hydrophilic groups, as determined by the area under the curve between 265 and 282 eV, strongly increases on 'more dense' PVMS networks, hence those, made of PVMS chains with a lower molecular weight. Note that the peak height at 268 eV is approximately the same for both molecular weights. We note that a similar observation, namely that the UVO treatment produced more hydrophilic species on lower molecular weight material, was recently also seen in PDMS networks treated with UVO [59].

In our previous work on UVO-treated PDMS, we studied the dependence of the surface wettability on the UVO-treatment time [30]. We reported that in order to generate a large number of hydrophilic functionalities on the surface of PDMS, one has to treat the PDMS specimens with UVO times in excess of 30 min. The production of surface hydrophilic moieties was accompanied with the formation of a ≈5 nm thick silica-like layer on top of the PDMS (density is ≈50% of silica). This stiff top-skin on the flexible PDMS foundation impeded the mobility of the surface groups. From the previous discussion, it is obvious short UVO-treatment times for PVMS lead to substantial changes in its surface chemistry. We took advantage of this brief exposure time, to limit the elasticity changes to PVMS-modified surface.

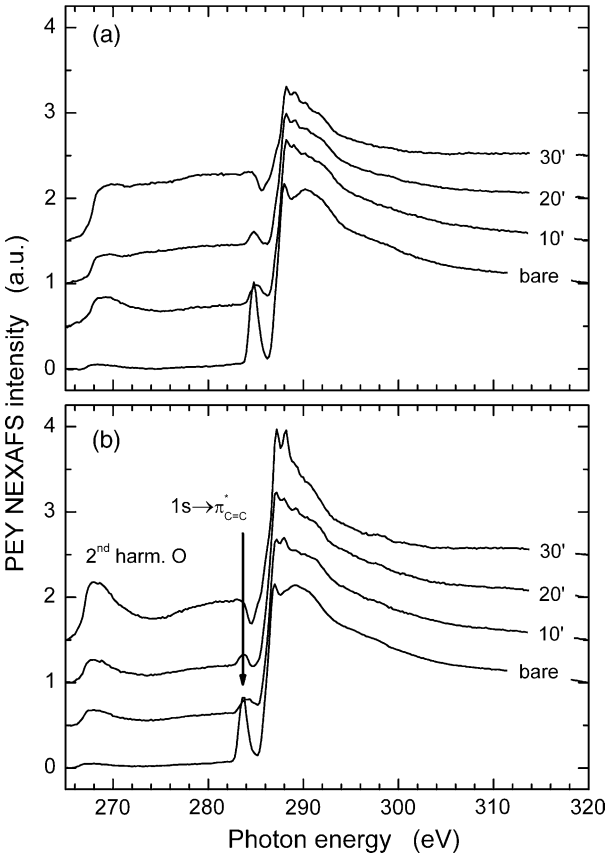

Fig. 4. Partial energy yield NEXAFS spectra at the carbon K-edge collected from for PVMS samples with $M_n = 34$ kDa (a) and $M_n = 49$ kDa (b) treated for various UVO times ranging from 0 to 30 min. The spectra have been shifted vertically for clarity.

The surface elasticity of PVMS-UVO material as a function of the UVO-treatment time was established from experiments utilizing atomic force microscopy indentation using a sharp AFM tip. In Fig. 5, we plot the normalized surface elastic modulus of the UVO-modified sample with respect to the bare PVMS specimen ($E_{PVMS\text{-}UVO}/E_{PVMS}$) as a function of the UVO-treatment times for PVMS with $M_n = 34$ kDa (open symbols) and $M_n = 54$ kDa (closed symbols). In both cases, the $E_{PVMS\text{-}UVO}/E_{PVMS}$ ratio increases with increasing UVO treatment times reaching apparent saturation only at very long times. We note that PVMS-UVO loses elasticity by a much weaker extent than PDMS-UVO, [31] where values as high as 80 were observed for $E_{PVMS\text{-}UVO}/E_{PVMS}$ for similar treatment times. From the data in Fig. 5, PVMS with higher molecular weight exhibits larger $E_{PVMS\text{-}UVO}/E_{PVMS}$. This observation is perhaps a bit surprising given the fact that the lower molecular weight PVMS networks were seen to be more effective in generating a large number of the hydrophilic surface moieties. Work is currently in progress to elucidate further this behavior. Here we offer a tentative explanation. From the data in Fig. 5, the surface modulus is almost the same for both molecular weights at short UVO times. This suggests that the primary mechanism involved in the interaction of

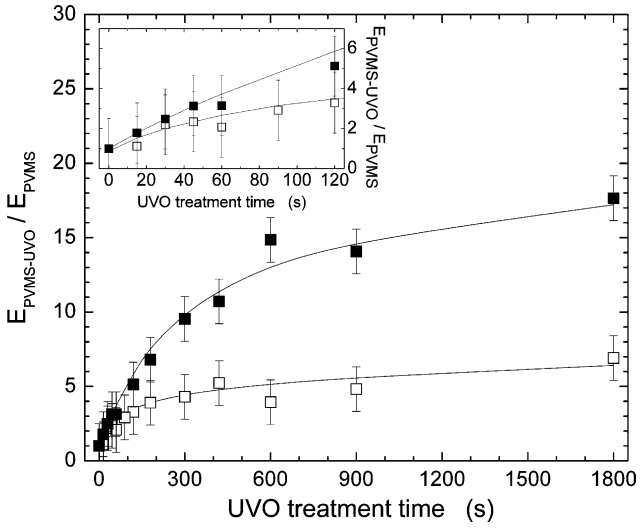

Fig. 5. Ratio of the elastic surface-moduli of UVO-treated PVMS ($E_{PVMS\text{-}VO}$) and bare PVMS (E_{PVMS}) as a function of the UVO treatment time. The measurements were performed for PVMS samples with $M_n = 34$ kDa (open symbols) and $M_n = 54$ kDa (closed symbols).

UVO with PVMS is the conversion of the vinyl groups. From the previous discussion recall, that vinyl groups are more susceptible to UVO relative to the Si–O–Si bonds. With increasing UVO time, Si–O–Si bonds scission starts to occur. Koberstein and coworkers established that the Si–O–Si linear linkages are more stable than linkages involving multiple oxygens bound to a single Si atom [29]. Hence, the cross-link points of the network will likely be attacked first by the UVO. Considering that the concentration of cross-link points increases with decreasing molecular weight of PVMS, lower molecular weight PVMS network will undergo more chain scission at the cross-link points. At longer UVO times, the low molecular weight PVMS will also have a higher mobility and thus lower chance to form cross-links from activated vinyl groups. In contrast, the higher molecular weight PVMS will be less mobile and will have a chance to form cross-links between neighboring activated vinyl groups. A higher cross-link density in the higher molecular weight PVMS with increasing UVO time would explain the higher surface modulus. Clearly more work is needed to fully understand the difference in surface modulus change with PVMS molecular weight.

Overall, the indentation experiments revealed that only minor changes to the PVMS surface modulus occurred for short UVO treatment times. In fact, considering the experimental error, the PVMS-treated and PVMS-bare modulus values are comparable during the first 2 min of the UVO treatment time. These results confirm that short UVO treatment time does not markedly alter the PVMS bulk elasticity, and thus the functional groups residing on these PVMS-UVO surfaces should possess adequate mobility to respond to environmental changes.

We have tested the responsiveness of the PVMS-UVO surfaces by depositing a droplet of water and measuring the

time evolution of the contact angle. In Fig. 6 we present images of the water droplet deposited on PVMS-UVO surface treatment for various UVO times (ordinate) and collected the images at increasing time intervals after depositing the droplet (abscissa). The number in the corner of each image represents the contact angle evaluated by assuming that the droplet forms a hemisphere and that the contact angle is the tangent to the drop at the water/substrate/air interface. The data in Fig. 6 confirm our previous findings, namely that increasing UVO time leads to enhanced hydrophilicity of the PVMS-UVO surfaces. For all UVO treatment times, there is a further decrease in the water contact angle with increasing exposure time to water. Based on the short 30 s water exposure times, the decrease in water contact angle is not due to evaporation of water from the probing droplet. Apparently, the surfaces of the PVMS-UVO samples rearrange in response to the presence of water and expose a large number of hydrophilic moieties to the sample/water interface. This behavior is a consequence of the high mobility of the PVMS polymer backbone, which remains relatively unmodified by the UVO treatment, as indicated by the modulus data in Fig. 5.

We have also tested the reversibility of this effect. Specifically, after exposing the surfaces to water, which led to the aforementioned decrease in the water contact angle, we have removed the water droplet by a Kimwipe and re-exposed the surface to the water droplet. The contact angles were on average ≈10–15° lower than measured on completely dried samples. Drying the sample surfaces with a stream of dry nitrogen helped to increase the contact angles but they still remained ≈5° lower than measured on completely dried samples. Vacuum drying and mild annealing (≈60 °C) also did not lead to a complete recovery of the original contact angle. Apparently some traces of water remained trapped inside the sub-surface layer and could not be removed by any of the above treatments. Further investigation is under way to completely understand the recovery process in such systems and results will be published in a separate publication [60].

In order to further verify the efficiency of the UVO treatment of PVMS relative to that of PDMS, we have formed self-assembled monolayers (SAMs) by depositing semifluorinated dimethylchlorosilanes, *m*-F8H2, and trichlorosilanes, *t*-F8H2 on PVMS and PDMS substrates activated with various UVO treatment times. The rational behind these experiments was that higher concentration of the hydrophilic functionalities on the SE surface should lead to higher grafting densities of the F8H2 molecules. Moreover, by carrying out the experiment with both mono- and tri-functional organosilanes, we should be able to also address the nature of bonding of the SAM molecules to the surface. Specifically, while *m*-F8H2 can only attach to the surface as a single molecule, the *t*-F8H2 can form two-

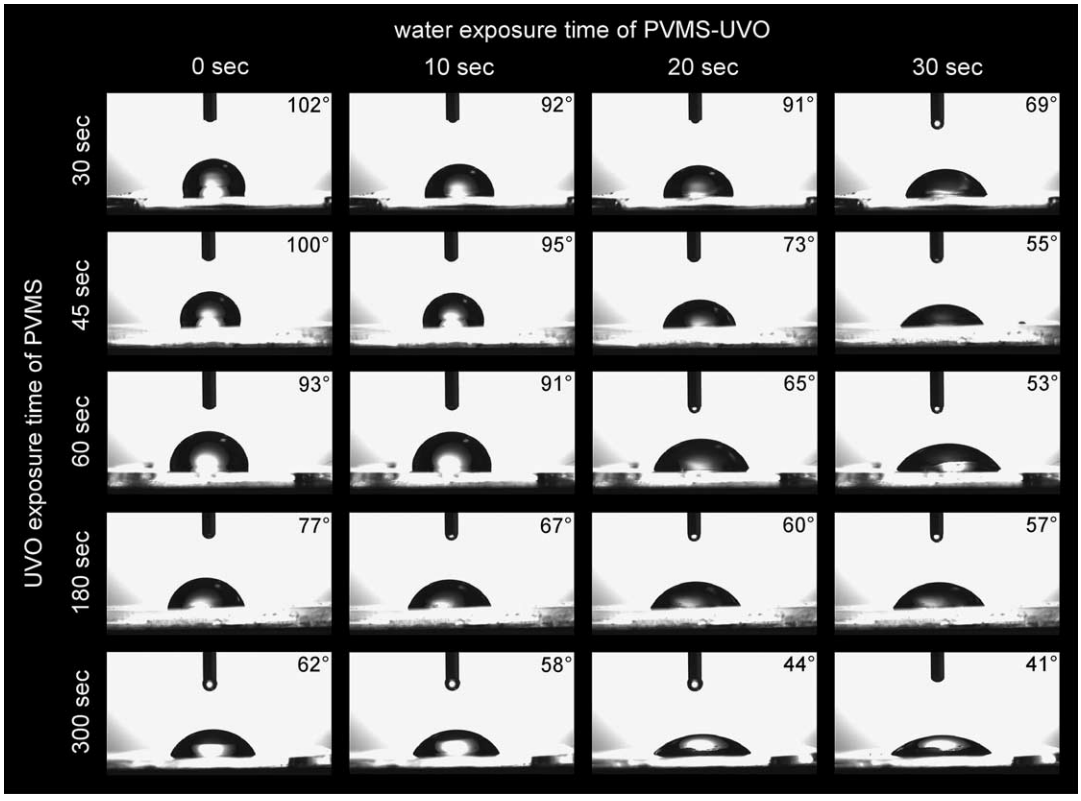

Fig. 6. Images of water droplet spreading on PVMS-UVO surfaces treated for various UVO times (ordinate) collected at various time intervals after depositing the droplet (abscissa). The numbers indicate the water contact angle that was evaluated from the images of the water droplets.

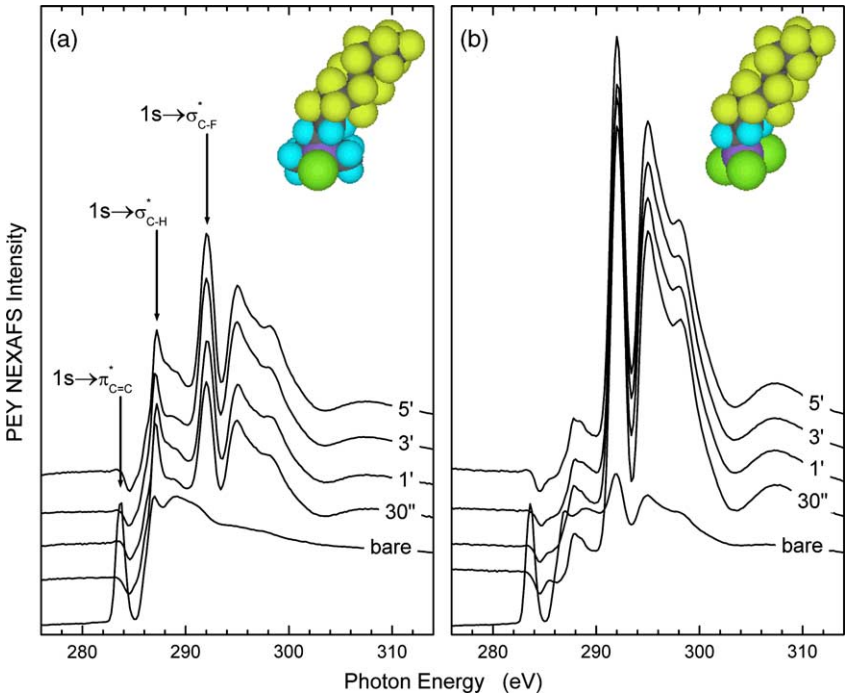

Fig. 7. Partial energy yield NEXAFS spectra at the carbon K-edge collected from for *m*-F8H2 (a) and *t*-F8H2 (b) SAMs deposited on PVMS network films (M_n = 39 kDa) that were previously treated for various UVO treatment times. The arrows indicate the positions of the characteristic NEXAFS transitions. See text for details. Also shown are cartoons illustrating the molecular structure of *m*-F8H2 and *t*-F8H2.

dimensional in-plane networks. Hence, in the latter case, one may expect to see relatively high concentration of the *t*-F8H2 molecules on surfaces that contain only a small number of attachment points.

We used the partial electron yield (PEY) signal in NEXAFS spectroscopy to monitor the chemistry variation on the surfaces of the samples. In Fig. 7 we plot the PEY NEXAFS spectra at the carbon K-edge *m*-F8H2 (a) and *t*-F8H2

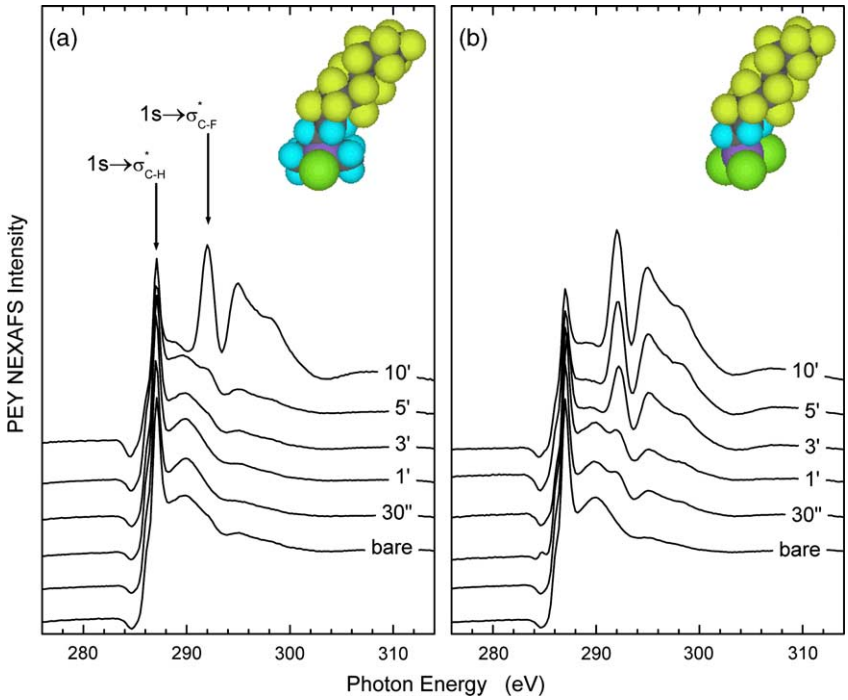

Fig. 8. Partial energy yield NEXAFS spectra at the carbon K-edge collected from for *m*-F8H2 (a) and *t*-F8H2 (b) SAMs deposited on PDMS network films (M_n = 39 kDa) that were previously treated for various UVO treatment times. The arrows indicate the positions of the characteristic NEXAFS transitions. See text for details. Also shown are cartoons illustrating the molecular structure of *m*-F8H2 and *t*-F8H2.

(b) SAMs deposited on PVMS network films treated for various UVO times. The data collected from the *m*-F8H2/PVMS-UVO sample reveal that no monolayer is formed on untreated PVMS. However, the appearance of the peak at 292 eV, which is a characteristic signature of a $1s \rightarrow \sigma^*$ transition of the C–F bond, in samples treated for as short as 30 s indicates that *m*-F8H2 molecules were bound to the PVMS-UVO substrate. Interestingly, *t*-F8H2 deposited on bare PVMS was able to form a monolayer, albeit rather poorly organized. We tentatively explain this by considering the assumption we have made, namely that the *t*-F8H2 molecules first form an in-plane network, which then gets physisorbed onto the PVMS surface. Further increase in the UVO treatment time resulted in a large concentration of fluorine and hence a higher grafting density of *m*-F8H2 in the SAM. The structure of the *t*-F8H2 molecules deposited on PVMS substrates exposed briefly to UVO is very different from that of *m*-F8H2 on the bare PVMS substrate. Specifically, the spectra shown in Fig. 7(b) are almost identical to those seen on dense *t*-F8H2 SAMs on silica [61]. Hence only short exposure times for PVMS were needed to generate a large enough number of surface active sites capable of forming organized SAMs from both *m*-F8H2 and *t*-F8H2 molecules.

In Fig. 8, we plot PEY NEXAFS spectra collected from *m*-F8H2 (a) and *t*-F8H2 (b) SAMs deposited on PDMS network films treated for various UVO times. As the spectra reveal, the SAM formation on PDMS-UVO is very different from that on PVMS-UVO. Specifically, first traces of an incomplete *m*-F8H2 SAM are detected for PDMS substrates treated for at least 5 min. Hence even 10-fold longer treatment times still do not lead to well-organized arrays of *m*-F8H2 molecules on PDMS-UVO. Only UVO times in excess of 10 min are capable of generating a large enough number of the surface hydrophilic functionalities that can be used a grafting sites for the *m*-F8H2 moieties.

In contrast to the deposition on bare PVMS, no traces of *t*-F8H2 molecules are seen on untreated PDMS substrates. While we still expect that the molecules would form an in-plane stabilized network, this cannot be physisorbed to the rather-hydrophobic substrate. Only after treating the PDMS substrate for 30 s enough attachment points are created to anchor the *t*-F8H2 network. A more complete *t*-F8H2 SAM is formed on PDMS when UVO treated in excess of 3 min. Even after 10 min of UVO treatment time, the number density of the *t*-F8H2 SAM on the PDMS-UVO materials is still much lower than that of the *t*-F8H2 SAM on the PVMS-UVO treated for 30 s.

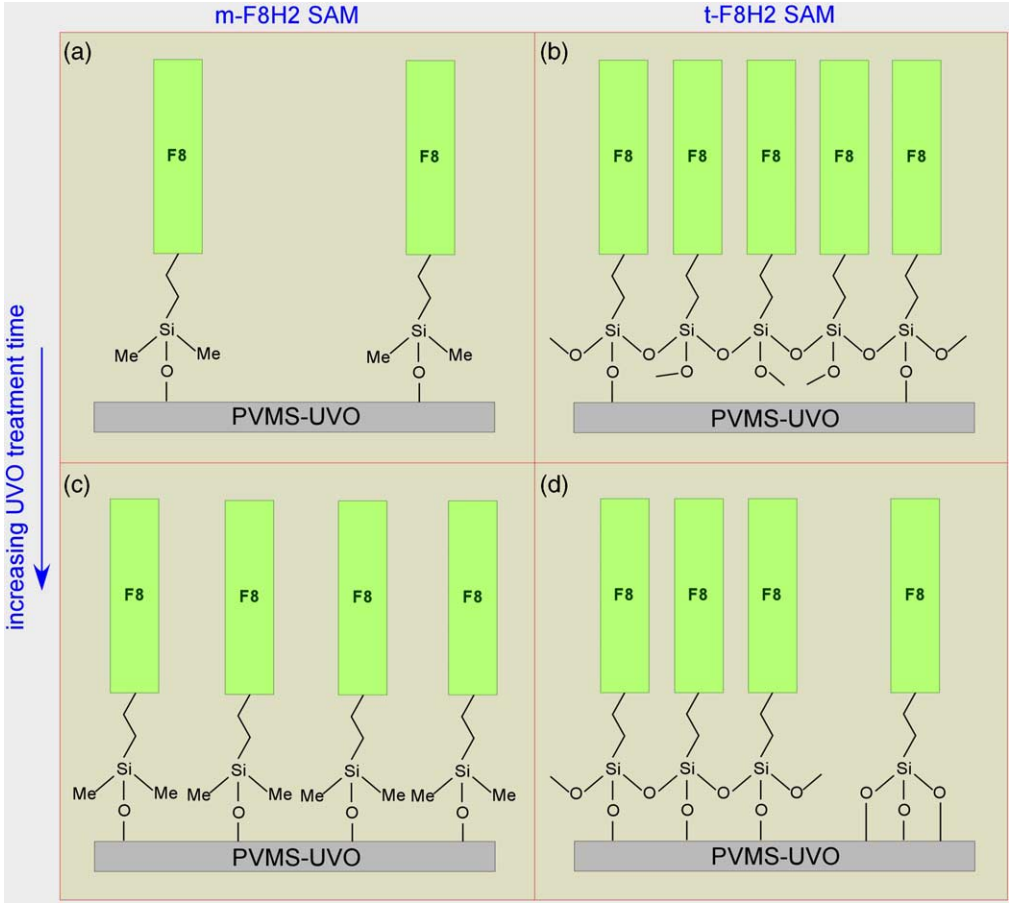

Fig. 9. Schematic illustrating the organization of monolayes of monofunctional silanes [*m*-F8H2, (a) and (c)] and trifunctional silanes [*t*-F8H2, (b) and (d)] on PVMS-UVO surfaces, realized by PVMS exposed to UVO for short (a) and (b), and for long (c) and (d), treatment times.

Fig. 9 summarizes our findings with regard to the formation of SAMs from mono- and tri-functionalized organosilanes on UVO-treated silicone elastomer surfaces. At short UVO-treatment time, only a few grafting sites are generated on the surface. While *m*-F8H2 organosilanes only form sparsely dense SAMs, *t*-F8H2 SAMs deposit in higher coverages mainly because they form an in-plane cross-linked networks. Increasing the UVO time leads to a large number of grafting points on the silicone elastomer surface. As a consequence, the concentration of both *m*-F8H2 and *t*-F8H2 increases.

4. Conclusions

In this work we reported on rapid generation of hydrophilic silicone elastomer surfaces by utilizing UV/ozone treatment of poly(vinylmethyl siloxane) (PVMS) network films. We demonstrated that UVO treatment causes oxidation of the vinyl groups in PVMS and that this oxidation leads to hydrophilic moieties, mainly surface-bound hydroxyls. Increasing the UVO treatment time increases both the concentration of the hydrophilic groups and the surface modulus of the network material. Short UVO exposure (up to 2 min) does not cause dramatic increases in the surface hardness. The PVMS-UVO surfaces retain their softness and are capable of responding to outside environmental change; they become more hydrophilic when exposed to a hydrophilic medium, such as water. We have also confirmed that UVO-activated surfaces are capable of organizing SAMs of organosilane molecules. UVO-activated PVMS is more effective in generating densely populated semifluorinated SAMs than UVO-activated PDMS. Importantly, for this to occur, only 30 s UVO treatment times are needed to activate the PVMS surface. Our results also provide evidence that while mono-functionalized silanes can only attach directly to the substrate, SAMs of tri-functionalized organosilanes form in-plane networks that are anchored to the underlying substrates.

Acknowledgements

We gratefully acknowledge the financial support from Sealed Air Cryovac, Office of Naval Research and the National Science Foundation (NER Program).

References

[1] Koberstein JT, editor. 'Polymer surfaces and interfaces', a collection of articles published in the MRS Bulletin, vol. 21, 1996. p. 16–53 [No. 1].
[2] Russell TP. Science 2002;297:964.
[3] Koberstein JT. Tailoring polymer interface properties by end group modification in polymer surfaces interfaces and thin films series on directions in condensed matter physics. Singapore: World Publishing; 2000. p. 115–81 [and references therein].
[4] Koberstein JT. Encyclopedia of polymer science and technology. New York: Wiley; 2001 [and references therein].
[5] Anastasiadis SH, Retsos H, Pispas S, Hadjichristidis N, Neophytides S. Macromolecules 2003;36:1994.
[6] Carey DH, Ferguson GS. Macromolecules 1994;27:7254.
[7] Carey DH, Ferguson GS. J Am Chem Soc 1996;118:9780.
[8] Carey DH, Grunzinger SJ, Ferguson GS. Macromolecules 2000;33:8802.
[9] Khongtong S, Ferguson GS. J Am Chem Soc 2001;123:3588. Khongtong S, Ferguson GS. Macromolecules 2002;35:4023.
[10] Khongtong S, Ferguson GS. J Am Chem Soc 2002;124:7254.
[11] Hedden RC, Saxena H, Cohen C. Macromolecules 2000;33:8676.
[12] Clarson SJ. Depolymerization, degration and thermal properties of siloxane polymers. In: Clarson SJ, Semlyen JA, editors. Siloxane polymers. Englewood Cliffs, NJ: Prentice Hall; 1993. p. 216–44.
[13] Owen MJ. 'Siloxane surface activity', in silicon-based polymer science: A comprehensive resource. In: Zeigler JM, Gordon Fearon FW, editors. Advances in chemistry series, vol. 24.
[14] Wynne K, Ho T, Johnston E, Myers S. Appl Organomet Chem 1998;12:763.
[15] Thanawala SK, Chaudhury MK. Langmuir 2000;16:1256 [and references therein].
[16] Chaudhury MK. J Adhes Sci Technol 1993;7:669. Chaudhury MK. Biosens Bioelectron 1995;10:785.
[17] Hillborg H, Gedde UW. IEEE Trans Dielect Electr Insul 1999;6:703.
[18] Liston EM, Martinu L, Wertheimer MR. In: Strobel M, Lyons C, Mittal, editors. Plasma surface modification of polymers: Relevance to adhesion. Utrecht: VSP; 1994. p. 3.
[19] Strobel M, Walzak MJ, Hill JM, Lin A, Karbashewski E, Lyons CS. In: Mittal KL, editor. Polymer surface modification: Relevance to adhesion. Utrecht: VSP; 1996. p. 233.
[20] Vaidya A, Chaudhury MK. J Colloid Interface Sci 2002;249:235.
[21] Thanawala SK, Chaudhury MK. Langmuir 2000;16:1256 [and references therein].
[22] Ferguson GS, Chaudhury MK, Biebuyck H, Whitesides GM. Macromolecules 1993;26:5870.
[23] Owen MJ, Smith PJ. J Adhes Sci Technol 1994;8:1063.
[24] Hillborg H, Anker JF, Gedde UW, Smith GD, Yasuda HK, Wilström K. Polymer 2000;41:6851.
[25] Vasilets VN, Nakamura K, Uyama Y, Ogata S, Ikada Y. Polymer 1998;39:2875.
[26] Ishii M, Komatsubara M. 1998 IEEE conference on electrical insulation and dielectric phenomena, Atlanta, USA 1998. p. 134.
[27] Huck TSW, Bowden N, Onck P, Pardoen T, Hutchinson JW, Whitesides GM. Langmuir 2000;16:3497.
[28] Koberstein JT, Mirley CL. US Patent No. 5,661,092; 1997; Koberstein JT, Mirley CL. US Patent No. 5,962,079; 1999.
[29] Ouyang M, Yuan C, Muisener RJ, Boulares A, Koberstein JT. Chem Mater 2000;12:1591.
[30] Efimenko K, Wallace WE, Genzer J. J Colloid Interface Sci 2002;254:306.
[31] Efimenko K, Rackaitis M, Manias E, Vaziri A, Mahadevan L, Genzer J. Nature Materials 2005;4:293.
[32] Cai G, Weber WP. Polymer 2002;43:1753.
[33] Kossmehl G, Fluthwedel A, Schafer H. Makromol Chem Makromol Symp 1992;193:2289.
[34] Choinovski J, Cypryk M. Synthesis of linear polysiloxane. In: Jones RG, Ando W, Choinovski J, editors. Synthesis of linear polysiloxane, vol. 3. Dordrecht: Kuwer Academic Publishers; 2000.
[35] Bostick EE. Ordered organopolysiloxanes, US Patent 3,337,497; 1967.
[36] Formoy TR, Semleyen JA. Polym Commun 1989;30:86.
[37] Choinovski J. In: Clarson SJ, Semlyen SA, editors. Siloxane polymers. Englewood Cliffs, NJ: Ellis Horwood/PTR Prentice Hall; 1993.
[38] Suzuki T, Okawa T. Polymer 1988;29:2095.
[39] Suzuki T. Polymer 1989;30:333.

[40] Chojnowski J, Rozga K. J Inorg Organomet Polym 1992;2:297.
[41] Patel SK, Malone C, Cohen JR, Gilmore JR, Colby RH. Macromolecules 1992;25:5241.
[42] Certain commercial equipment is identified in this article in order to specify adequately the experimental procedure. In no case does such identification imply recommendation or endorsement by the National Institute of Standards and Technology, nor does it imply that the items identified are necessarily the best available for the purpose.
[43] For detailed information about the NIST/Dow soft X-ray materials characterization facility at NSLS BNL, see: http://nslsweb.nsls.bnl.gov/nsls/pubs/newsletters/Nov96/Dow.html.
[44] Fischer DA, Mitchell GE, Yeh AT, Gland JL. Appl Surf Sci 1998;133:58. Genzer J, et al. Langmuir 2000;16:1993.
[45] Stöhr J. NEXAFS spectroscopy. Berlin: Springer; 1992.
[46] Due to the nature of the polarization dependencies of the NEXAFS signal intensities one cannot distinguish between a completely disoriented sample and a sample, whose chains are all tilted by $\approx 55°$, the so called, 'magic angle'.
[47] By carrying the NEXAFS experiments at $\theta = 55°$ we wanted to eliminate any possible influence of the orientation of the various functional groups at the SE surface on the PEY NEXAFS intensity. Several data sets collected at various angles θ indeed confirmed that these surface functionalities were not oriented.
[48] Manias E, Chen J, Fang N, Zhang X. Appl Phys Lett 2001;79:1700.
[49] Radmacher M, Fritz M, Cleveland JP, Walters DA, Hansma PK. Langmuir 1994;10:3809.
[50] Rotsch C, Radmacher M. Langmuir 1997;13:2825.
[51] Chizhik SA, Huang Z, Gorbunov VV, Myshkin NK, Tsukruk VV. Langmuir 1998;14:2606.
[52] Uilk JM, Mera AE, Fox RB, Wynne KJ. Macromolecules 2003;36.
[53] Scibiorek M, Gladkova NK, Chojnowski J. Polym Bull 2000;44:377.
[54] Herczynska L, Lestel L, Boileau S, Chojnowski J, Polowinski S. Eur Polym J 1999;35:1115.
[55] RozgaWijas K, Chojnowski J, Zundel T, Boileau S. Macromolecules 1996;29:2711.
[56] RozgaWijas K, Chojnowski J, Boileau S. J Polym Sci, Part A: Polym Chem 1997;35:879.
[57] Anderson DR. In: Smith AL, editor. The analysis of silicones. New York: Wiley; 1974. p. 247.
[58] Delman AD, Landy M, Simms BB. J Polym Sci A 1969;7:3375.
[59] Efimenko K, Genzer J, Vorvolakos K, Chaudhury MK. In preparation.
[60] Crowe JA, Efimenko K, Schwark DW, Genzer J. Responsive siloxane-based polymeric surfaces, in: Minko S, editor, Responsive Polymer Materials, Blackwell Professional Publishing, in press, 2005.
[61] Genzer J, Efimenko K, Fischer DA. Langmuir 2002;18:9307.